

***d*-wave superconductor as a model of high- $T_c$  superconductors**

Hyekyung Won\* and Kazumi Maki

*Department of Physics, University of Southern California, Los Angeles, California 90089-0484*

(Received 9 July 1993)

We study the bulk properties of *d*-wave superconductors relevant to high- $T_c$  copper oxides within weak-coupling theory. The superfluid density, the tunneling conductance, and the frequency-dependent electric conductivity appear to be quite consistent with some of the experimental data from single crystals of  $\text{YBa}_2\text{Cu}_3\text{O}_7$  and  $\text{Bi}_2\text{Sr}_2\text{CaCuO}_8$ . We also predict strong anisotropy in the ultrasonic attenuation when a sound wave is propagated within the *a*-*b* plane.

**I. INTRODUCTION**

Since the discovery of high- $T_c$  superconducting copper oxides by Bednorz and Müller,<sup>1</sup> tremendous efforts have been invested to understand the mechanism and the nature of high- $T_c$  superconductors. However, it appears that we are still far from understanding the basic mechanism involved in superconducting pairing.<sup>2</sup> Recently a possible  $d_{x^2-y^2}$  wave superconductor in  $\text{YBa}_2\text{Cu}_3\text{O}_7$  and other high- $T_c$  oxides has been considered rather seriously.<sup>3-6</sup> The *d*-wave model describes not only the almost absence of the coherence peak in  $T_1^{-1}$  the nuclear-spin-lattice relaxation rate<sup>7</sup> but also the suppression of the superconducting transition temperature when Cu in the  $\text{CuO}_2$  plane is replaced by Zn, Ni, etc.<sup>8,9</sup> More recently the angle-resolved photoemission from the  $\text{Br}_2\text{Sr}_2\text{CaCuO}_8$  (BSCCO) crystal by Shen *et al.*<sup>10</sup> indicates that the photoemission spectra is consistent with  $d_{x^2-y^2}$  superconductor. Therefore, it is gratifying if  $d_{x^2-y^2}$ -wave superconductor follows from the two-dimensional Hubbard model as recent Monte Carlo analysis suggests.<sup>5,6</sup>

The object of this paper is to study systematically the bulk properties of the *d*-wave superconductors within the weak-coupling model.<sup>13</sup> In order to represent the layered structure common to copper oxides, we take the Fermi surface as a cylinder with axis parallel to the *c* axis. Then the  $d_{x^2-y^2}$  superconducting order parameter is written as  $\Delta(k) = \Delta f$  with  $f = \cos(2\phi)$ , where  $\phi$  is the angle the quasiparticle momentum, which lies in the *a*-*b*-plane, makes from the *a* axis. Perhaps we have to mention a more recent angle-resolved photoemission data by Kelley

*et al.*,<sup>11</sup> which suggests a *d*-wave superconductor but with different symmetry from above  $\Delta(k)$ . Indeed this form of *d*-wave superconductor has been suggested<sup>12</sup> for the superconductor in the Bechgaard salts and this type of the order parameter has also an advantage in avoiding the strong on-site Coulomb potential. For this alternative *d*-wave model, we have  $f = \cos(ck_3)$ . The lines of zeros in the superconducting energy gap for these two models are shown in Figs. 1(a) and 1(b), respectively. Following the BCS paper,<sup>14</sup> we study both thermodynamics and the transport properties of these two *d*-wave superconductors.<sup>15</sup> Indeed, the above two *d*-wave superconductors give identical thermodynamics, the density of states, the superfluid density, and the frequency-dependent electric conductivity are not easily distinguishable. In addition to the above-mentioned photoemission spectra, the angle dependence of the ultrasonic attenuation coefficient can discriminate between these alternative *d*-wave models.

**II. GAP EQUATION AND THERMODYNAMICS**

Within the weak-coupling model, the gap equation is given by<sup>16</sup>

$$\lambda^{-1} = 2\pi T \langle |f|^2 \rangle^{-1} \sum_n \left\langle \frac{|f|^2}{\sqrt{\omega_n^2 + \Delta^2 |f|^2}} \right\rangle \tag{1}$$

with  $f = \cos(2\phi)$  or  $\cos(ck_3)$  and  $\langle \rangle$  means average over the Fermi surface,  $\lambda$  is the dimensionless coupling constant,  $\omega_n$  is the Matsubara frequency and the sum over  $\omega_n$  is cutoff at  $\omega_n = \epsilon_c$ . It is more convenient to rewrite Eq. (1) as

$$-\ln \left[ \frac{\Delta(T)}{\Delta(0)} \right] = 2 \langle |f| \rangle^{-1} \int_0^\infty dE (1 + e^{\beta E})^{-1} \times \langle |f|^2 \text{Re}(E^2 - \Delta^2 |f|^2)^{-1/2} \rangle \\ = \frac{8}{\pi} \int_0^\infty dx (1 + e^{\beta \Delta x})^{-1} \{ \theta(x-1)x[K(x^{-1}) - E(x^{-1})] + \theta(1-x)[K(x) - E(x)] \}, \tag{2}$$

where  $K(k)$  and  $E(k)$  are the complete elliptic integrals. Here  $\beta = T^{-1}$  and the order parameter at  $T=0$   $K$  is given by

$$\Delta(0) = \frac{\pi}{\gamma} T_c e^c \tag{3}$$

with

$$C = - \langle |f|^2 \rangle^{-1} \langle |f|^2 \ln |f| \rangle = \ln 2 - \frac{1}{2} \cong 0.1931472 \dots \tag{4}$$

and  $\gamma = 1.7810 \dots$  is the Euler constant. This gives

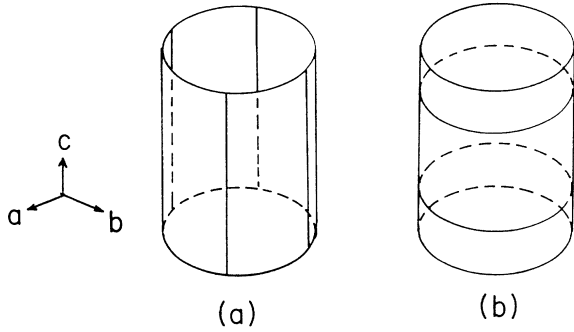


FIG. 1. The lines of zeros in the superconducting energy gap are shown for two types of *d*-wave superconductors (a)  $f = \cos(2\phi)$ , (b)  $f = \cos(ck_3)$ .

$$\Delta(0)/\Delta_{\text{BCS}}(0) = 1.21306 \dots \quad (5)$$

The gap equation (2) is solved numerically and  $\Delta(T)/\Delta(0)$  is shown in Fig. 2 as function of  $t = T/T_c$  together with the one for the *s*-wave superconductor.<sup>14</sup> Except for a somewhat larger value of  $\Delta(0)$ ,  $\Delta(T)/\Delta(0)$  behaves quite similar to the *s*-wave one. From  $\Delta(T)$  the thermodynamical critical field  $H_c(T)$  and specific heat are easily obtained. We show in Figs. 3 and 4,  $D(T)$  the deviation from the parabolic law,

$$D(T) = H_c(T)/H_c(0) - [1 - (T/T_c)^2] \quad (6)$$

and the specific heat as function of  $t^2$  and  $t$ , respectively. In particular  $D(T)$  is almost twice as large as the one for the *s*-wave superconductor. We note that the order parameter deduced from the tunneling conductance of BSCCO (Refs. 17 and 18), for example, gives much larger  $\Delta(0)$  [ $\Delta(0)/\Delta_{\text{BCS}}(0) = 2.13$ ].

### III. DENSITY OF STATES AND TUNNELING CONDUCTANCE

The electron density of states is readily obtained from

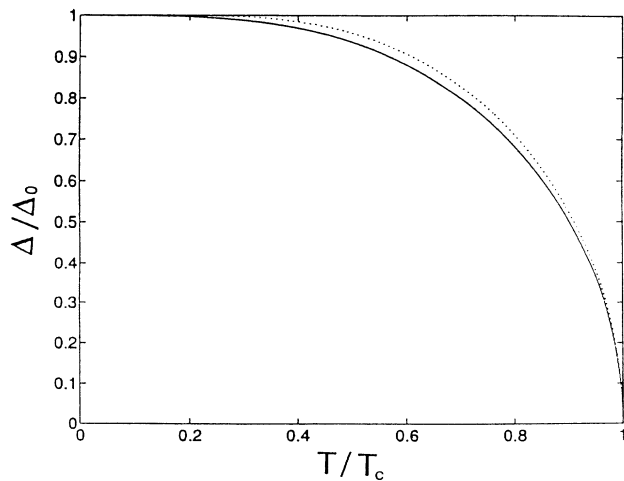


FIG. 2. The superconducting order parameter  $\Delta(T)$  is shown as function of the reduced temperature  $t = T/T_c$ . Here  $\Delta_0 = \Delta(0)$  and the broken curve is for the *s*-wave superconductor.

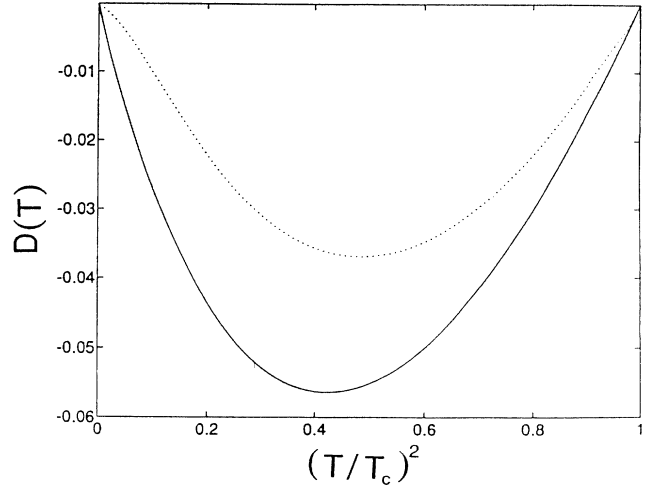


FIG. 3. The deviation from the parabolic law is shown for *d*-wave (—) and *s*-wave (· · · ·) superconductors.

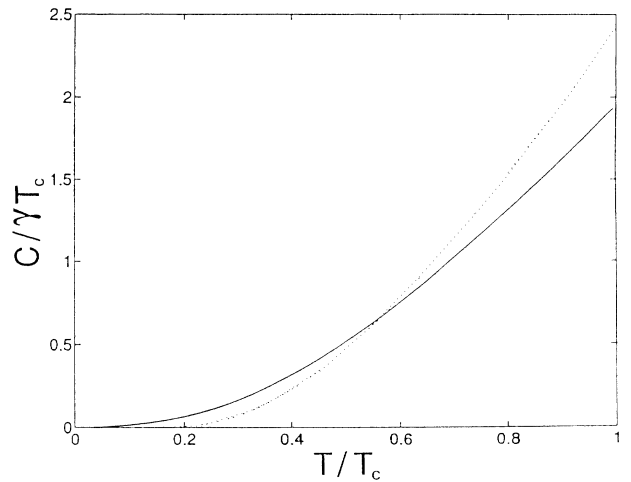


FIG. 4. The specific heat is shown as function of  $T/T_c$  for *d*-wave (—) and *s*-wave (· · · ·) superconductors.

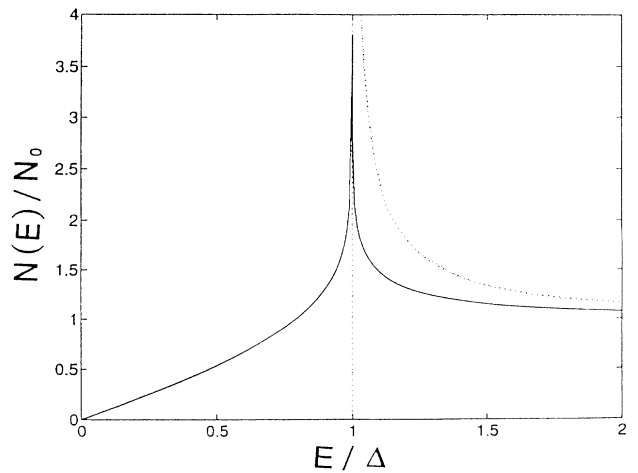


FIG. 5. The density of states is shown for *d*-wave (—) and *s*-wave (· · · ·) superconductors.

$$N(E)/N_0 = \left\langle \text{Re} \left[ \frac{E}{\sqrt{E^2 - \Delta^2 |f|^2}} \right] \right\rangle$$

$$= \begin{cases} \frac{2}{\pi} x K(x) & \text{for } x \leq 1 \\ \frac{2}{\pi} K(x^{-1}) & \text{for } x > 1, \end{cases} \quad (7)$$

where  $x = E/\Delta$  and  $K(x)$  is the complete elliptic integral. Equation (7) is evaluated numerically and shown in Fig. 5. The density of states has a logarithmic peak at  $E = \Delta$ . Also  $N(E)$  increases linearly with  $E$  for small  $E/\Delta$ . From Eq. (7) the tunneling conductance between superconductor and normal metal and between two superconductors is given by

$$G_{sn}(eV)/G_{nn} = e^{-1} \frac{d}{dV} \left\{ N_0^{-1} \int_{-\infty}^{\infty} dE N(E) \{f(E - eV) - f(E)\} \right\} = \frac{1}{4} \beta N_0^{-1} \int_{-\infty}^{\infty} dE N(e) \text{sech}^2(\frac{1}{2}\beta(E - eV)) \quad (8)$$

and

$$G_{ss}(eV)/G_{nn} = e^{-1} N_0^{-2} \frac{d}{dV} \left\{ \int_{-\infty}^{\infty} dE N(E) N(E - eV) \{f(E - eV) - f(E)\} \right\}$$

$$= N_0^{-2} \int_{-\infty}^{\infty} dE N(E - eV) \left\{ \frac{\beta}{4} N(E) \text{sech}^2 \left[ \frac{1}{2} \beta E \right] + \frac{\partial N(E)}{\partial E} [f(E - eV) - f(E)] \right\}, \quad (9)$$

respectively, where  $f(E) = (1 + e^{\beta E})^{-1}$ . These conductances are shown in Figs 6 and 7, respectively. At low temperatures the tunneling conductance increases almost quadratically with  $eV$  and have a peak at  $eV = 2\Delta(T)$  and then the normalized conductance drops almost to unity. This behavior is qualitatively similar to the conductance observed in  $\text{Bi}_2\text{Sr}_2\text{CaCu}_2\text{O}_3$  by the break-junction technique.<sup>17,18</sup> However, a detailed comparison reveals a few significant differences. First, the temperature dependence of the order parameter which is identified by the peak position of the conduction is quite different. The order parameter deduced from the observed conductance depends much weakly on the temperature. Further the observed peak value of the conductance is much larger (almost by a factor of 2) then predicted theoretically. Finally there is a small dip just outside of the peak, which is not in the theory. These features appear to indicate the necessity of the strong-coupling theory.

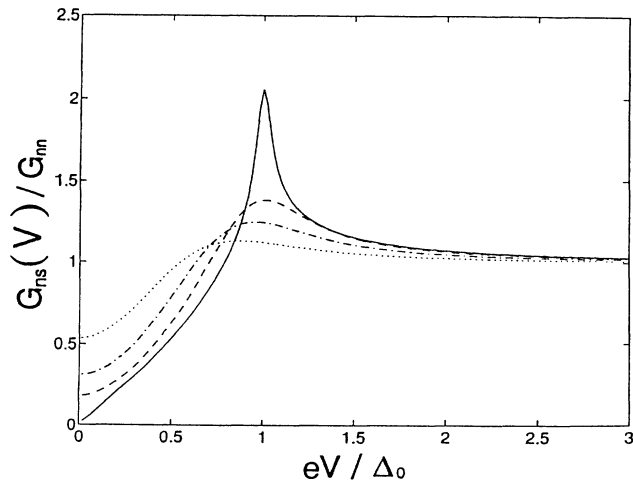


FIG. 6. The tunneling conductance between normal and superconducting are shown for  $T/T_c = 0.06$  (—),  $0.5$  (---),  $0.7$  (-·-·-), and  $0.861$  (····).

#### IV. SUPERFLUID DENSITY AND ELECTRIC CONDUCTIVITY

It is easily seen that the temperature dependence of the superfluid density is completely isotropic and the same for the two  $d$ -wave models we are considering, though the superfluid density itself is anisotropic. So we have

$$\rho_s(T)/\rho = 2\pi T \sum_n \left\langle \frac{\Delta^2 |f|^2}{(\omega_n^2 + \Delta^2 |f|^2)^{3/2}} \right\rangle \quad (10)$$

$$= 1 - \frac{\beta}{\pi} \Delta \int_0^\infty dx \text{sech}^2(\frac{1}{2}\beta\Delta x)$$

$$\times [\theta(x-1)K(x^{-1}) + \theta(1-x)xK(x)]. \quad (11)$$

The superfluid density is evaluated numerically and shown in Fig. 8. In particular  $\rho_s(T)/\rho$  decreases linearly

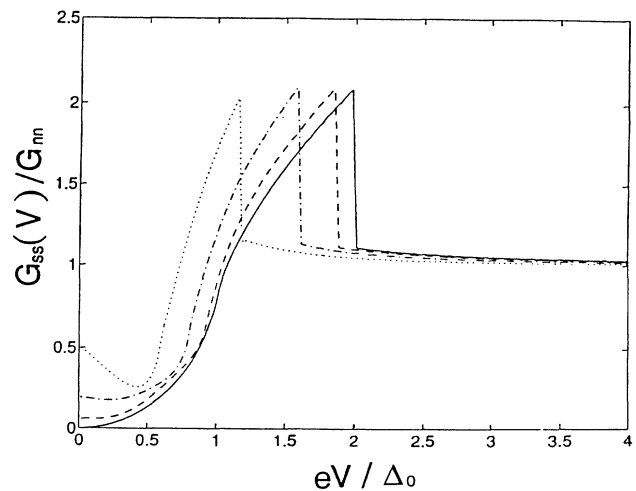


FIG. 7. The tunneling conductance between two superconductors are shown for  $T/T_c = 0.06$  (—),  $0.5$  (---),  $0.7$  (-·-·-), and  $0.86$  (····).

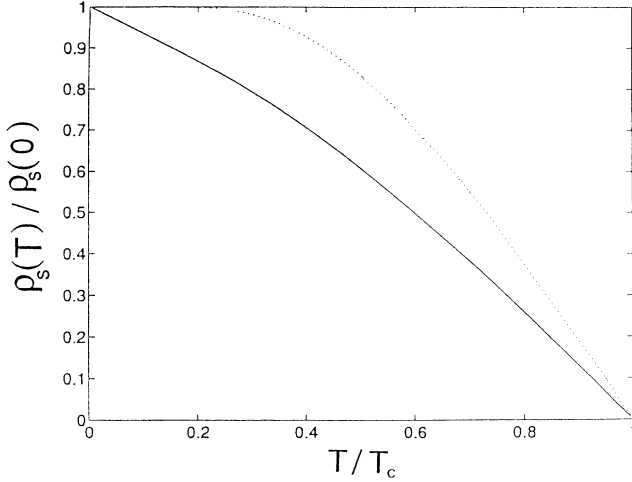


FIG. 8. The superfluid density is shown as function of  $T/T_c$  for  $d$ -wave (—) and  $s$ -wave (· · ·) superconductors.

in  $T$  at low temperature consistent with a recent measurement of  $\rho_s(T)/\rho$  of single crystals of YBaCuO by Hardy *et al.*<sup>19</sup> However, the observed linear slope is smaller roughly by a factor of  $\frac{3}{4}$  which indicates again larger  $\Delta(0)$  for YBaCuO as well. We note a similar but phenomenological curve is presented by Scalapino.<sup>20</sup> We note also

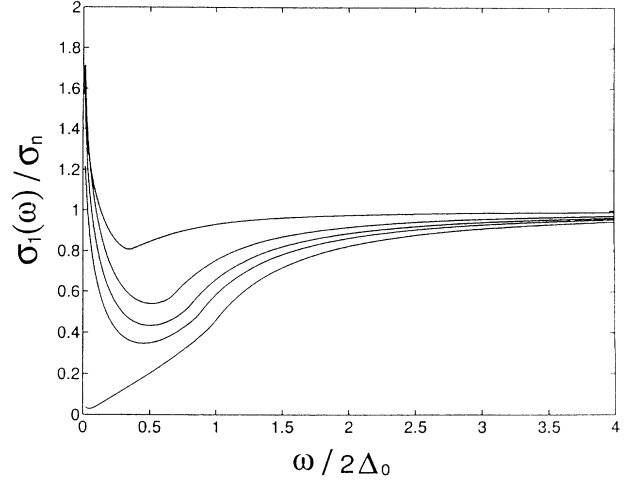


FIG. 9. The frequency-dependent electric conductivity is shown as function of  $\omega/2\Delta_0$  for  $T/T_c = 0.95, 0.8, 0.7, 0.6,$  and  $0.06$  from top to bottom.

the spin susceptibility in the superconducting state is given by  $\chi_s/\chi_n = 1 - \rho_s(T)/\rho$ . The frequency-dependent electric conductivity is also obtained by generalizing the Mattis and Bardeen result<sup>21</sup> for the  $d$ -wave superconductor. Especially at  $T=0$  K, we obtain

$$\frac{\sigma_1(\omega)}{\sigma_N} = \frac{8}{\pi} \left[ \frac{\omega}{2\Delta} \right] \left\{ \theta(\omega - 2\Delta) \int_{(\omega-2\Delta)/(\omega+2\Delta)}^1 dk \Phi(k) + \theta(2\Delta - \omega) \int_0^1 dk \Phi(k) \right\}, \quad (12)$$

where

$$\Phi(k) = (1+k)^{-2} [E(k) - (1-k)K(k)] \{ (1+k)^2 - (\omega/2\Delta)^2 (1-k^2) \}^{-1/2}. \quad (13)$$

For  $T \neq 0$  K, we have to use a more general expression

$$\sigma(\omega)/\sigma_N = \left\{ \left\langle \int_{\Delta|f|}^{\infty} d\omega' \frac{\omega'(\omega'+\omega) + \Delta^2|f|^2}{\{(\omega'^2 - \Delta^2|f|^2)[(\omega'+\omega)^2 - \Delta^2|f|^2]\}^{1/2}} \left[ \tanh \left[ \frac{\beta}{2}(\omega'+\omega) \right] - \tanh \left[ \frac{\beta}{2}\omega' \right] \right] \right\rangle \right. \\ \left. + \left\langle \int_{\Delta|f|}^{\omega - \Delta|f|} d\omega' \frac{\omega'(\omega - \omega') - \Delta^2|f|^2}{\{(\omega'^2 - \Delta^2|f|^2)[(\omega - \omega')^2 - \Delta^2|f|^2]\}^{1/2}} \tanh \left[ \frac{\beta}{2}\omega' \right] \right\rangle \right\} \omega^{-1}, \quad (14)$$

which can be transformed as integrals involving complete elliptic integrals. The frequency-dependent conductivity is calculated for a few temperatures and shown in Fig. 9. The result describes quite well the frequency-dependent conductivity of BSCCO determined by transmission measurements and reported by Mandras *et al.*<sup>18</sup> Especially at low temperature and at low frequency the conductivity increases linearly with  $\omega$ . We note, however, that the above expression is derived for either  $\lambda \ll \xi$  or  $l \ll \xi$  of which neither applies for high- $T_c$  copper oxides. Here  $\lambda$ ,  $\xi$ , and  $l$  are the penetration depth, the coherence distance, and the electron mean free path, respectively. On the opposite limit (i.e.,  $l\lambda \gg \xi$ ) indeed the electric conductivity becomes extremely small and develops a cusplike feature at  $\omega = 2\Delta(T)$ , which does not resemble the observation.<sup>22</sup>

## V. THERMAL CONDUCTIVITY AND THE ULTRASONIC ATTENUATION

Similarly the temperature dependence of the electronic thermal conductivity is isotropic. We obtain

$$\kappa^e(T)/\kappa_n^e(T) = 3(2\pi^2 T^3)^{-1} \int_0^{\infty} dE E^2 \langle \theta(E - \Delta|f|) \rangle \text{sech}^2 \left[ \frac{1}{2}\beta E \right] \\ = 1 - \frac{12}{\pi^2} (\beta\Delta)^2 \int_0^1 dx x \left[ 1 - \frac{2}{\pi} \sin^{-1} x - \frac{1}{\pi} \frac{x}{\sqrt{1-x^2}} \right] (1 + e^{\beta\Delta x})^{-1}, \quad (15)$$

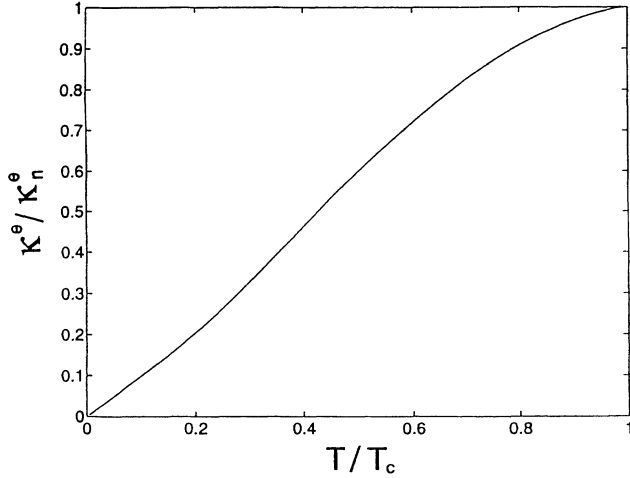


FIG. 10. The reduced thermal conductivity is shown as function of  $T/T_c$ .

which is shown in Fig. 10 as function of the reduced temperature. If the thermal conductivity is due to impurity scattering at low temperatures, this will give  $\kappa^e(t) \propto T^2$  at low temperatures. So far we described transport coefficients, which cannot discriminate the two  $d$ -wave superconductors. Here let us consider the ultrasonic attenuation coefficient.

(a)  $\mathbf{q} \parallel \mathbf{c}$  when the propagation vector is parallel to the  $c$  axis. The temperature dependence of the attenuation coefficient is independent of the direction of the polarization vector for the  $d_{x^2-y^2}$  state and given by

$$\begin{aligned} \alpha(T)/\alpha_n &= \frac{\beta}{2} \int_0^\infty dE \operatorname{sech}^2 \left[ \frac{\beta}{2} E \right] \langle \theta(E - \Delta|f|) \rangle \\ &= \frac{4}{\pi} \int_0^1 \frac{dx}{\sqrt{1-x^2}} (1 + e^{\beta\Delta x})^{-1} = a(T), \end{aligned} \quad (16)$$

while for  $f = \cos(ck_3)$ , the temperature dependence is different depending on the transverse and the longitudinal wave.

(b)  $\mathbf{q} \perp \mathbf{c}$  when the propagation vector lies in the  $a$ - $b$  plane. Further when the polarization vector lies in the  $a$ - $b$  plane with an angle  $\theta$  from the  $a$  axis, the attenuation coefficients for the  $d_{x^2-y^2}$  state are given as

$$\alpha^L(\theta)/\alpha_N = a(T) - \cos(4\theta)b(T) \quad (17)$$

and

$$\alpha^T(\theta)/\alpha_N = a(T) + \cos(4\theta)b(T) \quad (18)$$

for the longitudinal and the transverse wave, respectively, where  $a(T)$  has been already defined in Eq. (16) and

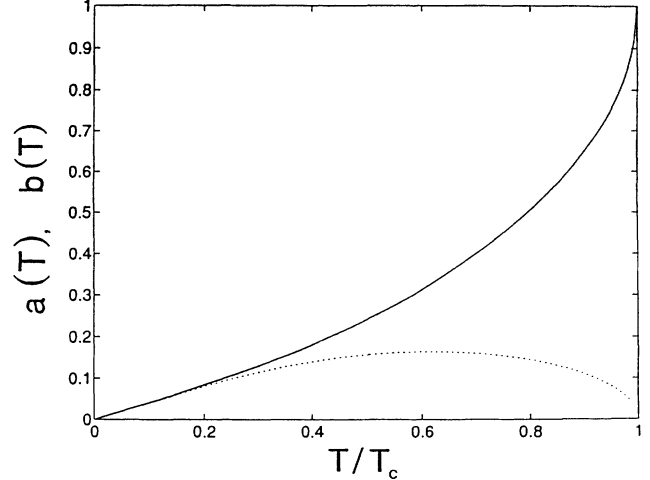


FIG. 11. Two coefficients describing the ultrasonic attenuation coefficient  $a(T)$  (—) and  $b(T)$  (· · · ·) are shown as function of  $T/T_c$ .

$$b(T) = \frac{4}{\pi} \int_0^1 dx \frac{(1-2x^2)}{\sqrt{1-x^2}} (1 + e^{\beta\Delta x})^{-1}. \quad (19)$$

The temperature dependence of  $a(T)$  and  $b(T)$  are shown in Fig. 11. Since  $a(T) \cong b(T)$  at low temperatures ( $T \leq 0.2T_c$ ), the ultrasonic attenuation coefficients are strongly anisotropic at low temperature. For the transverse wave with  $\mathbf{e}$  (the polarization vector)  $\parallel \mathbf{c}$ , the attenuation coefficient is again Eq. (16).

## VI. CONCLUDING REMARKS

We have studied two types of  $d$ -wave superconductors, which are thought relevant to high- $T_c$  copper oxides. We find that both thermodynamic properties and most of transport coefficients cannot discriminate between these two candidates. Therefore at the present moment the angle-resolved photoemission experiment has a clear advantage in discriminating these two states. Perhaps also the anisotropy in the nmr relaxation time<sup>23</sup> may discriminate these two states, but we do not want to enter into this question at this moment.

## ACKNOWLEDGMENTS

We have benefited from an enlightening discussion with Gene Bickers and Doug Scalapino. We also thank Laszlo Mihaly for sending us a copy of Ref. 18 prior to publication. One of us (H.W.) thanks the Korean Science and Engineering Foundation for travel support. This present work was supported by the National Science Foundation under Grant No. DMR 92-18317.

\*On leave from Physics Department, Hallym University, Chunchon 200-702, South Korea.

<sup>1</sup>J. G. Bednorz and K. A. Müller, Z. Phys. B **64**, 189 (1986).

<sup>2</sup>P. W. Anderson and J. R. Schrieffer, Phys. Today **44** (June), 54 (1991); B. Goss Levi, Phys. Today **46** (May), 17 (1993).

<sup>3</sup>N. E. Bickers, D. J. Scalapino, and S. R. White, Phys. Rev.

Lett. **62**, 961 (1989).

<sup>4</sup>P. Monthoux, A. Balatsky, and P. Pines, Phys. Rev. Lett. **67**, 3448 (1991).

<sup>5</sup>N. Bulut and D. J. Scalapino, Phys. Rev. Lett. **67**, 2898 (1991).

<sup>6</sup>N. Bulut, D. J. Scalapino, and S. R. White, Phys. Rev. B **47**, 14 599 (1993).

- <sup>7</sup>M. Takigawa *et al.*, Phys. Rev. E **44**, 7764 (1991); J. Martindale *et al.*, Phys. Rev. Lett. **68**, 702 (1992).
- <sup>8</sup>Gang Xiao *et al.*, Phys. Rev. B **42**, 8752 (1990); H. Adrian and S. Nielsen, Europhys. Lett. **5**, 265 (1988).
- <sup>9</sup>R. J. Radtke, K. Levin, H. B. Schüttler, and M. R. Norman, Phys. Rev. B **48**, 653 (1993).
- <sup>10</sup>Z.-X. Shen *et al.*, Phys. Rev. Lett. **70**, 1553 (1993).
- <sup>11</sup>R. J. Kelley, Jian Ma, G. Margaritondo, and M. Onellion (unpublished).
- <sup>12</sup>Y. Hasegawa and H. Fukuyama, J. Phys. Soc. Jpn. **56**, 877 (1987); Y. Suzumura and H. J. Schulz, Phys. Rev. B **39**, 11 398 (1989).
- <sup>13</sup>H. Won and K. Maki, Physica B (to be published).
- <sup>14</sup>J. Bardeen, L. N. Cooper, and J. R. Schrieffer, Phys. Rev. **108**, 1175 (1957).
- <sup>15</sup>See for a parallel analysis of *d*-wave superconductors relevant to heavy-fermion superconductors; M. Brinkmeier and K. Maki (unpublished).
- <sup>16</sup>P. W. Andeson and P. Morel, Phys. Rev. **123**, 1911 (1961).
- <sup>17</sup>D. Mandrus, L. Forro, D. Keller, and L. Mihaly, Nature (London) **351**, 460 (1991).
- <sup>18</sup>D. Mandrus, J. Hartge, C. Kendziora, L. Mihaly, and L. Forro, Europhys. Lett. **22**, 199 (1993).
- <sup>19</sup>W. N. Hardy, D. A. Bonn, D. C. Morgan, R. Liang, and K. Zhang, Phys. Rev. Lett. **70**, 3999 (1993).
- <sup>20</sup>D. J. Scalapino (unpublished).
- <sup>21</sup>D. C. Mattis and J. Bardeen, Phys. Rev. **117**, 912 (1958).
- <sup>22</sup>K. Maki and H. Won (unpublished).
- <sup>23</sup>J. P. Lu, Mod. Phys. Lett. B **6**, 547 (1992).